

# Manipulation of Zeeman coherence in solids at room temperature: Ramsey interference in the coherent-population-trapping spectrum of ruby

Roman Kolesov, Marlan O. Scully, and Olga Kocharovskaya

*Department of Physics, Texas A&M University, College Station, Texas 77843-4242, USA*

(Received 11 September 2006; published 22 November 2006)

Coherent population trapping (CPT) in a three-level atomic medium pumped by two subsequent short optical pulses is considered under the condition of negligible population decay from the excited optical state. It is shown that the amount of atomic population transferred to the excited state by the combined action of the pulses strongly depends on the phase of the ground-state coherence excited by the first pulse at the arrival time of the second pulse. Oscillatory behavior of optical excitation efficiency on the time delay between the pulses is predicted. It is also shown that saturating optical pulses can produce population inversion in a resonantly pumped quasi-two-level system. A class of solid materials in which the predicted phenomena can be observed at room temperature is found. It includes some rare-earth and transition-metal doped dielectric crystals where Orbach relaxation between ground-state Zeeman states is suppressed: ruby, alexandrite, and several others. On the basis of the theoretical predictions, experimental observation of Ramsey fringes in CPT spectrum of ruby is reported.

DOI: [10.1103/PhysRevA.74.053820](https://doi.org/10.1103/PhysRevA.74.053820)

PACS number(s): 42.50.Gy, 42.50.Nn, 78.20.Ls

## I. INTRODUCTION

Ramsey interference is one of the most significant applications of atomic coherence [1]. It can be viewed as a double-slit experiment in which the magnitude and the phase of atomic coherence excited at the initial instant of time and location affects interaction with the coherent electromagnetic wave at a later time and, possibly, at a different location. The interference pattern is very similar to the one typically observed in a double-slit experiment in which the time interval between the interaction instants serves as a distance between the slits. Ramsey interference allows one to read out the complete state of atomic coherence including its amplitude and phase. This feature is of great importance for quantum information processing since it allows us to retrieve the state of a qubit.

Though the first experimental demonstration of Ramsey fringes was performed with separated oscillatory magnetic fields, Ramsey interference can be observed in spectra of coherent population trapping (CPT, Ref. [2]) by all-optical means. Several groups reported their results obtained in alkali-metal atomic beams [3] and vapor cells [4]. In these experiments, Ramsey interference resulted in extremely narrow optical transmission and absorption resonances (of the order of a few Hz). Another interesting effect related to Ramsey interference is the so-called diffusion-induced Ramsey narrowing of CPT resonance [5]. In both cases, the ultimate goal of the research was to detect ultranarrow optical resonances for use in atomic clocks. Ramsey interference can be also observed by Faraday rotation of optical polarization in a situation when the atomic beam passes through two spatially separated laser beams, of which the first creates spin coherence and the second one probes it [6]. Faraday rotation of the probe laser beam is an extremely sensitive tool of studying the amplitude and the phase of spin coherence in the collision-free situation. Apart from the atomic beam and vapor experiments, some important results on the realization of Ramsey interference have been achieved in solid media, such

as quantum dots [7], and even in electrical circuits based on a superconducting tunnel junction [8]. However, so far no experimental results have been reported on Ramsey interference in solids at room temperature.

In the present paper, we present the theoretical analysis of Ramsey interference in room-temperature optical crystals doped with either transition-metal or rare-earth ions and its experimental observation in the coherent population trapping (CPT) spectrum of ruby. The main idea of the present work is to excite the coherence between Zeeman sublevels of the ground state by an optical pulse, then let the coherence evolve for some time, and then test its state by applying another optical pulse. Thus we study the line shape of the CPT spectrum of a  $\Lambda$ -type medium under the action of two optical pulses as it was done in works [4,5]. The peculiarity of room-temperature solids is that the lifetime of ground-state Zeeman coherence is much shorter than the population decay from the excited optical state. Thus excitation of ground-state coherence cannot rely on the populating of so-called “dark” state by population decay (see [9]). In the next section, we consider a simplified three-level theoretical model showing how Zeeman coherence excited by the first optical pulse affects the absorption of the second one under the condition of no population decay from the excited optical state. It is shown that Ramsey interference can result in a population inversion under resonant pumping of a quasi-two-level medium. In Sec. III, the class of solid materials, in which Ramsey interference in CPT spectra can be observed at room temperature, is identified. Significant reduction of Orbach relaxation rate between Zeeman or hyperfine ground-state components for certain transition-metal and rare-earth ions doped into optical crystals makes these materials suitable for optical creation and manipulation of Zeeman coherence. Experimental observation of modulation of CPT spectrum of ruby due to Ramsey interference is presented in Sec. IV. Finally, the most important results are summarized in Sec. V.

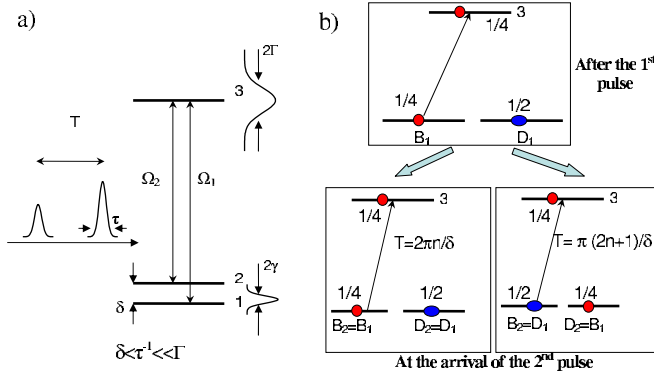


FIG. 1. (Color online) (a) Three-level model of a medium interacting with two optical pulses separated by time interval  $T$ . (b) Two situations are considered for saturating optical pulses: (i) the second pulse arrives at  $T=2\pi n/\delta$ ; it cannot pump the medium since the transition  $|B_2=B_1\rangle \leftrightarrow |3\rangle$  is already saturated by the first pulse; (ii) the second pulse arrives at  $T=\pi(2n+1)/\delta$ ; it can excite more atoms because “bright” and “dark” states flipped, i.e.,  $|B_2\rangle=|D_1\rangle$  and  $|D_2\rangle=|B_1\rangle$ .

## II. CPT IN A THREE-LEVEL MEDIUM UNDER EXCITATION BY TWO SUBSEQUENT ULTRASHORT PULSES

Let us consider interaction of a three-level atomic medium with two optical ultrashort pulses of duration  $\tau \ll \delta^{-1}$ , where  $\delta$  is the frequency splitting between Zeeman sublevels 1 and 2, and time interval  $T \gg \tau$  between them [see Fig. 1(a)]. The following assumptions will be used: (i) there is no population decay from the excited optical state 3 at the time scale of interest; (ii) dipole moments of both optical transitions  $1 \leftrightarrow 3$  and  $2 \leftrightarrow 3$  are equal,  $\mu_{31}=\mu_{32}=\mu$ , and assumed to be real and positive; (iii) optical transitions are homogeneously broadened with half linewidth being  $\Gamma$  and  $\Gamma^{-1}$  is the shortest time scale in the problem; (iv) Zeeman transition  $1 \leftrightarrow 2$  is homogeneously broadened with half linewidth being  $\gamma \ll \tau^{-1}$ ; (v) the initial populations of the two ground-state sublevels are equal. These assumptions reflect the real physical parameters of the transition-metal and rare-earth doped optical crystals mentioned above. We will be interested in the amount of population transferred into level 3 under the combined action of optical pulses. The following notations will be used:  $\hbar\delta$  is the energy separation between the ground-state sublevels  $\rho_{nm}$ ,  $n=1, 2, 3$  is the population of the  $n$ th level, and  $\sigma$  is the complex amplitude of the ground-state coherence. The electric field in the optical wave is defined as follows:

$$E = \sum_{n=1}^2 \{ \mathcal{E}_n [t - (n-1)T] e^{-i\omega t} + \text{c.c.} \} / 2. \quad (1)$$

Here  $\mathcal{E}_{1,2}(t)$  are the complex amplitudes of the electric field in the two pulses and  $\omega$  is the carrier frequency. The amplitudes  $\mathcal{E}_{1,2}(t)$  are essentially nonzero only for  $|t|, |t-T| < \tau$ . The efficiency of interaction of the pulses with the medium is defined by their Rabi frequency,  $\Omega_{1,2}(t) = \mu \mathcal{E}_{1,2}(t) / 2\hbar$ .

First of all, we examine how the first pulse interacts with the medium. We assume that its duration is shorter than the

oscillation period of Zeeman transition, i.e.,  $\tau \ll 2\pi\delta^{-1}$ . The latter condition means that each optical pulse couples the excited state 3 with a “bright” coherent superposition of Zeeman sublevels [2] defined as follows:

$$|B_1\rangle = \frac{1}{\sqrt{2}}(|1\rangle + |2\rangle). \quad (2)$$

Index 1 indicates that we are dealing with the bright state during the action of the first pulse. Optical excitation from the bright state is determined by the matrix element  $\langle 3|\hat{\mu}|B_1\rangle = \sqrt{2}\mu$ . The coherent superposition orthogonal to  $|B_1\rangle$ , the so-called “dark” state, is defined as follows:

$$|D_1\rangle = \frac{1}{\sqrt{2}}(|1\rangle - |2\rangle). \quad (3)$$

It is not involved in the excitation process since the dipole matrix element  $\langle 3|\hat{\mu}|D_1\rangle = 0$ . Initially, both  $|B_1\rangle$  and  $|D_1\rangle$  are equally populated as the pure energy levels 1 and 2:  $\rho_{B_1 B_1} = \rho_{D_1 D_1} = \rho_{11} = \rho_{22} = 1/2$ . Due to very strong homogeneous broadening of the optical transitions, both pulses act as an optical pumping with the instantaneous pumping rate  $P_{1,2}(t) = 8\Omega_{1,2}^2(t)/\Gamma$ . The final population of level 3 after the action of the first pulse is given by the following expression:

$$\rho_{33} = \frac{1}{4}(1 - x_1), \quad x_1 = \exp\left(-\int_{-\infty}^{\infty} P_1(t) dt\right). \quad (4)$$

Correspondingly, the population of the bright state is  $\rho_{B_1 B_1} = (1+x_1)/4$ . One sees that the optical pulse tends to equalize  $\rho_{33}$  and  $\rho_{B_1 B_1}$ .

Let us first examine the situation when decoherence between Zeeman sublevels is absent [see Fig. 1(b)]. During the time interval between the pulses, the coherent superpositions of states, being initially bright and dark, evolve according to the following formulas:

$$|S_1\rangle(t=0) = |B_1\rangle, \quad |S_2\rangle(t=0) = |D_1\rangle, \quad (5)$$

$$|S_1\rangle = \frac{1}{\sqrt{2}}(|1\rangle + e^{-i\delta t}|2\rangle), \quad |S_2\rangle = \frac{1}{\sqrt{2}}(|1\rangle - e^{-i\delta t}|2\rangle). \quad (6)$$

It is clear that the bright state gradually becomes dark and vice versa. However, populations of  $|S_1\rangle$  and  $|S_2\rangle$  do not change. If the second pulse arrives at the instant of time corresponding to the whole period of oscillations at the Zeeman transition, the corresponding bright and dark states are exactly the same as during the action of the first pulse:  $|B_2\rangle = |S_1(t=2\pi n/\delta)\rangle = |B_1\rangle$  and  $|D_2\rangle = |S_2(t=2\pi n/\delta)\rangle = |D_1\rangle$ . In this case, the second pulse tends to equalize the populations of states  $|B_2\rangle$  and 3 with the initial conditions being  $\rho_{B_2 B_2} = (1+x_1)/4$  and  $\rho_{33} = (1-x_1)/4$ . The resulting population of level 3 is given by the expression

$$\rho_{33}(T=2\pi n/\delta) = \frac{1}{4}(1-x_1x_2), \quad x_2 = \exp\left(-\int_{-\infty}^{\infty} P_2(t)dt\right). \quad (7)$$

Here  $n$  is an integer. The situation is different if the second pulse arrives at the time instant  $T=\pi(2n+1)/\delta$ . In this case,  $|B_2\rangle=|S_2[t=\pi(2n+1)/\delta]\rangle=|D_1\rangle$  and  $|D_2\rangle=|S_1[t=\pi(2n+1)/\delta]\rangle=|B_1\rangle$  therefore the initial conditions are  $\rho_{B_2B_2}=1/2$  and  $\rho_{33}=(1-x_1)/4$ . The population of level 3 after the second pulse can be easily evaluated as follows:

$$\rho_{33}[T=\pi(2n+1)/\delta] = \frac{1}{2}\left[1 - \frac{1}{4}(1+x_1)(1+x_2)\right]. \quad (8)$$

The difference in the excitation efficiency in those two cases is given by

$$\begin{aligned} \Delta\rho_{33} &= \rho_{33}[T=\pi(2n+1)/\delta] - \rho_{33}(T=2\pi n/\delta) \\ &= \frac{1}{8}(1-x_1)(1-x_2). \end{aligned} \quad (9)$$

It is clear that the pair of pulses separated by  $T=\pi(2n+1)/\delta$  always excite more atoms than those separated by  $T=2\pi n/\delta$ . Thus one should expect oscillatory behavior of the excitation efficiency as the pulse temporal separation or the Zeeman transition frequency changes.

Let us consider the case of  $T=\pi(2n+1)/\delta$  more carefully. If both pulses saturate the optical transition, i.e.,  $\int_{-\infty}^{\infty} P_{1,2}(t)dt \gg 1$  and  $x_{1,2} \rightarrow 0$ , the final population of the excited optical state becomes  $\rho_{33}^{(fin)}=3/8$ . At the same time, populations of levels 1 and 2 are  $\rho_{11}^{(fin)}=\rho_{22}^{(fin)}=5/16 < \rho_{33}^{(fin)}$ . Thus the two pulses create population inversion at both  $1 \leftrightarrow 3$  and  $2 \leftrightarrow 3$  transitions. This is a nontrivial result, since both pulses effectively interact with two-level systems  $3 \leftrightarrow |B_{1,2}\rangle$ .

In order to take into account decoherence processes between Zeeman sublevels, the atomic medium has to be described using the density-matrix approach. Since both optical transitions are assumed to have the same dipole moment and homogeneous width, the populations of the two ground-state Zeeman sublevels are equal at all instants of time,  $\rho_{11}=\rho_{22}=\rho=(1-\rho_{33})/2$ . At the same time, complex amplitudes of the optical coherences  $\sigma_{31}$  and  $\sigma_{32}$  follow the amplitude of the optical field and can be evaluated algebraically in terms of  $\rho$  and  $\sigma$ , the ground-state coherence. Those two conditions allow one to reduce the whole set of six density-matrix equations to only two of them describing the behavior of  $\rho$  and  $\sigma$ :

$$\frac{d\rho}{dt} + P(t)[2(3\rho-1) + \sigma + \sigma^*] = 0, \quad (10)$$

$$\frac{d\sigma}{dt} + i\delta\sigma + 2P(t)(3\rho-1 + \sigma) = -\gamma\sigma. \quad (11)$$

Here  $P(t)=\Omega^2(t)/\Gamma$  is the pumping rate while  $\Omega(t)=\Omega_1(t)+\Omega_2(t-T)$ . Analytical calculations can be performed under the conditions  $\delta, \gamma \ll \tau^{-1}$ . In this case, we can neglect the terms responsible for oscillation and relaxation of the coherence during the action of each pulse. Thus after the first pulse

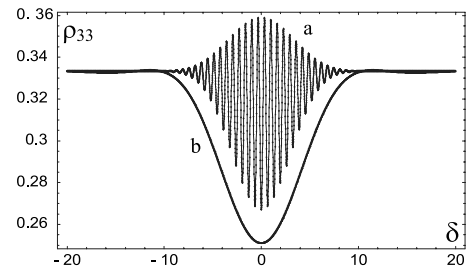


FIG. 2. Simulated CPT spectra: (a) under double-pulse excitation and (b) under single pulse excitation. The simulation parameters are  $\gamma=0.03$ , the shape of each pulse  $P(t)=10 \exp(-t^2/\tau^2)$ ,  $\tau=0.2$ , the distance between the pulses  $T=10$ .

the ground-state population and coherence become of the following form:

$$\rho^{(1)} = \frac{3+x_1}{8}, \quad \sigma^{(1)} = \frac{x_1-1}{8}, \quad (12)$$

with  $x_1$  being defined above. Before the arrival of the second pulse, populations of Zeeman sublevels remain the same while the ground-state coherence oscillates and decays:

$$\rho^{(1)'} = \frac{3+x_1}{8}, \quad \sigma^{(1)'} = \sigma^{(1)} \exp[-(i\delta + \gamma)T]. \quad (13)$$

These are the initial conditions describing the state of the medium before the arrival of the second pulse. Final populations of the ground-state Zeeman sublevels emerge from the set of equations (10) and (11) in the following form:

$$\begin{aligned} \rho^{(2)} &= \frac{1}{32}[11 + x_1 + x_2 + 3x_1x_2 + (1-x_1) \\ &\quad \times (1-x_2)e^{-\gamma T} \cos \delta T], \quad \rho_{33}^{(2)} = 1 - 2\rho^{(2)}. \end{aligned} \quad (14)$$

The amplitude of the interference term is proportional to  $\exp(-\gamma T)$ , as expected. The excitation efficiency is modulated as a function of Zeeman splitting.

The results of simulation of the set of equations (10) and (11) are presented in Fig. 2. The population of level 3 is plotted as a function of the ground-state splitting. The CPT spectrum corresponding to a single optical pulse is plotted for comparison. The above analytical description reproduces the results of simulation very well for  $\delta \ll \tau^{-1}$ .

It is possible to generalize the above analytical treatment for an arbitrary number of equidistant ultrashort pulses if each pulse saturates the optical transition. It is rather easy to show that after the  $n$ th pulse the excited-state population is given by the following expression:

$$\rho_{33}^{(n)} = \frac{1}{3} \left[ 1 - \frac{1}{4} \left( \frac{1 + 3 \exp(-\gamma T) \cos \delta T}{4} \right)^{n-1} \right]. \quad (15)$$

The resulting population of the excited level is also an oscillating function of the ground-state splitting though the widths of Ramsey interference resonances decrease as  $(n-1)^{-1/2}$  for  $\gamma=0$ . Thus the evolution of the CPT spectrum with the increase of the number of pulses is the following. A single ultrashort pulse produces a single level-crossing reso-

nance in zero magnetic field which is significantly broadened due to the short pulse duration [see Fig. 2(b)]. Two ultrashort pulses lead to harmonic modulation of the CPT resonance [see Fig. 2(a)]. With increase of the number of ultrashort pulses, this periodic modulation develops into a sequence of narrow CPT resonances within the original broad level-crossing resonance. The width of each resonance decreases as the number of pulses grows.

Noteworthy is that two limiting cases of a single broadened CPT resonance produced by a single ultrashort pulse and a series of CPT resonances produced by an infinite train of ultrashort pulses were studied earlier both theoretically and experimentally [9,10]. However, the general case of an arbitrary number of pulses and the intermediate case of several pulses (including the especially interesting case of two pulses) leading to periodic modulation of the single pulse CPT spectrum were not studied so far.

### III. ESTIMATES FOR SOLIDS AT ROOM TEMPERATURE

In the present section, it will be discussed how the phenomena discussed above can be observed in room-temperature solid media. The consideration will be focused on optical crystals doped with either transition-metal or rare-earth ions. The choice of the dopant ions is rather broad and includes most of those, in which electron paramagnetic resonance (EPR) can be observed at room temperature, i.e.,  $\text{Cr}^{3+}$ ,  $\text{Mn}^{2+}$ ,  $\text{Eu}^{2+}$ ,  $\text{Gd}^{3+}$ ,  $\text{Cu}^{2+}$ ,  $\text{Fe}^{3+}$ , and some others. All of them have an odd number of electrons in the open  $3d$  or  $4f$  shell and therefore they are Kramer's ions, i.e., all their electronic levels are spin doublets. The most important feature of these ions is large energy separation of the first excited electronic state from the ground one. This strongly reduces the contribution of resonant inelastic phonon scattering (so-called Orbach relaxation [11]) to spin dephasing and thus to EPR linewidth. The latter lies in the MHz–GHz range depending on the ion and crystalline host. However, in all these compounds the time of ground-state decoherence is much shorter than the time of population decay from the excited optical states (typically in the microsecond to millisecond range). Thus the mechanism of ground-state coherence excitation cannot be based on populating the dark state through spontaneous decay of the excited ions as is the case for alkali-metal vapors. In the following discussion, we consider two crystals, namely, ruby and alexandrite, and make estimates of the laser intensities and pulse delays required to observe previously discussed phenomena.

Ruby ( $\text{Cr}^{3+}:\text{Al}_2\text{O}_3$ ) is the most studied crystal in terms of its optical and EPR properties. The ground state of the  $\text{Cr}^{3+}$  ion has the total spin of  $3/2$  and consists of two spin doublets separated by  $0.38\text{ cm}^{-1}$  with  $\pm 1/2$  doublet lying above the  $\pm 3/2$  one (see Fig. 3). The ground state of the chromium ion in ruby is described by the following Hamiltonian:

$$H_{gs} = \mu_B(g_{\parallel}B_{\parallel}S_z + g_{\perp}\mathbf{B}_{\perp} \cdot \mathbf{S}_{\perp}) + D\left(S_z^2 - \frac{S(S+1)}{3}\right), \quad (16)$$

where  $\mu_B$  is Bohr magneton,  $g_{\parallel}=1.982$  and  $g_{\perp}=1.987$  are the ground-state  $g$  factors in the directions parallel and perpen-

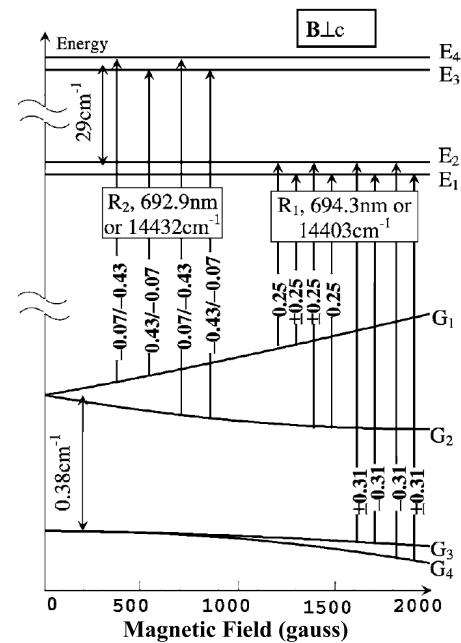


FIG. 3. Zeeman structure of electronic levels of  $\text{Cr}^{3+}$  in ruby. Splittings and optical polarization selection rules are indicated for  $\mathbf{B} \perp c$ . Optical transitions allowed for  $\sigma$  polarization of light propagating in the  $c$  direction are indicated by arrows connecting the corresponding energy levels accompanied by the corresponding matrix element. For the  $R_1$  line the upper/lower sign stands for  $\sigma^+/\sigma^-$  polarizations, respectively, while for the  $R_2$  line the first and second numbers correspond to  $\sigma^+$  and  $\sigma^-$ .

dicular to the crystal axis, respectively,  $2D = -11.47\text{ GHz}$  is the ground-state zero-field splitting, and  $B_{\parallel}$  and  $\mathbf{B}_{\perp}$  are the longitudinal and transverse magnetic-field components, respectively. The quantization axis is chosen to be along the crystal axis. Two lowest excited electronic states lie  $\sim 1.4 \times 10^4\text{ cm}^{-1}$  above the ground one. They give rise to two very well-known red lines in the optical emission and absorption:  $R_1$  (694.3 nm) and  $R_2$  (692.9 nm). Their linewidths at room temperature are  $\approx 11\text{ cm}^{-1}$  (full width at half maximum, FWHM) and the peak absorption cross section corresponding to the  $R_1$ -line absorption is  $2.5 \times 10^{-20}\text{ cm}^2$  [12]. The lifetime of excited states is 3 ms at room temperature and 4.3 ms at cryogenic temperatures. Since ruby has an internal symmetry axis, the optical selection rules strongly depend on the polarization of optical radiation. In addition, polarization selection rules for the transitions between particular Zeeman sublevels in the ground and in the excited states depend on the mutual orientation of the external magnetic field and the  $c$  axis [13]. The particular geometry of present interest is  $\mathbf{B} \perp c$  with the incident laser light being circularly polarized and propagating along the  $c$  axis as depicted in Fig. 3. In this geometry, there are two independent  $\Lambda$  systems formed by the two-photon optical transitions between the components of  $\pm 1/2$  and  $\pm 3/2$  doublets, respectively. Both  $\Lambda$  systems give rise to two overlapping CPT resonances in the vicinity of zero magnetic field [9]. Decoherence times at  $+1/2 \leftrightarrow -1/2$  and  $+3/2 \leftrightarrow -3/2$  Zeeman transitions are different because the former one is magnetic-dipole allowed while the latter one is forbidden. The direct measurements of coherence lifetimes

were performed in series of works [14,15] in which oscillatory behavior of optically induced magnetization (OIM) was studied under various excitation conditions and in various geometries. The longest lifetime was detected for the coherence excited between  $\pm 3/2$  sublevels of the ground state ( $\sim 20$  ns, Ref. [15]).

Let us make estimates of the laser intensity required to observe Ramsey fringes in the CPT spectrum related to Raman transition between  $\pm 3/2$  states. The pumping rate  $P(t)$  can be estimated on the basis of the absorption cross section  $\sigma_{abs}$  and photon flux  $\Pi(t)$  as  $P(t) = \Pi(t)\sigma_{abs} = I(t)\sigma_{abs}/\hbar\omega$ , where  $I(t)$  is the laser intensity. Correspondingly, the total excitation probability is given by  $\int P(t)dt = F\sigma_{abs}/\hbar\omega$  with  $F$  being the energy flux of the pulse. As was discussed in the previous section, Ramsey fringes are the most pronounced in case of saturating laser intensity, i.e., when  $\int P(t)dt > 1$ . Thus the required energy flux is  $F_{th} = \hbar\omega/\sigma_{abs} \approx 10$  J/cm<sup>2</sup>. According to the previous discussion, the time interval between the two pulses has to be shorter than the decoherence time, i.e., shorter than 20 ns. At the same time, each pulse should be much shorter than the time delay between them. Thus the optimal requirements for experimental observation of Ramsey fringes in ruby would be 100-ps–1-ns pulses delayed by 3–10 ns with the total-energy flux 5–10 J/cm<sup>2</sup>. The requirement for laser intensity can be relaxed by choosing another material with greater oscillator strength at the optical transition. One of the possible candidates would be alexandrite (Cr<sup>3+</sup>:BeAl<sub>2</sub>O<sub>4</sub>) where the maximum absorption cross section at the  $R_1$  line for chromium ions in mirror sites is  $\sim 1.5 \times 10^{-19}$  cm<sup>2</sup> [16], i.e., an order of magnitude larger than in ruby, while Zeeman decoherence parameters are the same as in ruby. In this case, the required laser flux is  $< 1$  J/cm<sup>2</sup>.

It is interesting to point out a possibility of creating population inversion at the  $R_2$  transition in ruby under pumping at the  $R_1$  transition. This up-conversion process can be used in laser cooling of crystals. Such a possibility is based on the fact that it is possible to excite two ground dark and bright states simultaneously by choosing the appropriate magnetic field and time interval between the two pulses. This fact allows one to exploit two ground-state coherences excited at  $+1/2 \leftrightarrow -1/2$  and  $+3/2 \leftrightarrow -3/2$  transitions. We assume that both optical pulses tend to saturate the  $R_1$  pumping transition. At room temperature, the populations of the two excited states of Cr<sup>3+</sup> ion equilibrate in a few picoseconds. Thus under or even 10–100-ps pumping the ratio of the two populations is fixed at all times and is equal to  $\exp(-D_{ex}/k_B\Theta) \approx 0.87$  for  $\Theta = 300$  K with population of the  $\bar{E}$  doublet being greater than that of the  $2\bar{A}$  one. Here  $D_{ex} = 29$  cm<sup>-1</sup> is the energy difference between  $\bar{E}$  and  $2\bar{A}$  levels,  $k_B$  is the Boltzmann constant, and  $\Theta$  is the temperature of the crystal. Let us consider the case when the ratio of the frequencies of the two ground-state Zeeman transitions  $+1/2 \leftrightarrow -1/2$  and  $+3/2 \leftrightarrow -3/2$  is an odd integer number. This can be done since the splitting of  $\pm 1/2$  levels is a linear function of the magnetic field while the frequency  $\omega_{+3/2 \leftrightarrow -3/2}$  is its cubic function. For a given number  $n$ , the magnetic field at which this ratio is equal to  $n$  is given by the following expression:

$$\frac{3}{8}D\left(\frac{\mu_B g_{\perp} B^*}{D}\right)^3 = 2\mu_B g_{\perp} B^*, \quad |B^*| = \frac{4}{\sqrt{3n}} \frac{|D|}{\mu_B g_{\perp}}. \quad (17)$$

The first optical pulse equalizes the populations of the two bright states

$$|B_1\rangle = (|+1/2\rangle + |-1/2\rangle)/\sqrt{2} \quad (18)$$

and

$$|B_2\rangle = (|+3/2\rangle + |-3/2\rangle)/\sqrt{2} \quad (19)$$

and those of the two Zeeman sublevels of the  $\bar{E}$  state. The initial populations of  $|B_{1,2}\rangle$  and the orthogonal dark states  $|D_{1,2}\rangle$  are equal to 1/4. We need to remember that  $\rho_{2\bar{A}2\bar{A}} = x\rho_{\bar{E}\bar{E}}$ ,  $x = 0.87$ . Thus after the first pulse  $\rho_{B_1 B_1} = \rho_{B_2 B_2} = \rho_{\bar{E}\bar{E}} = 1/4(2+x)$  while the populations of the two dark states do not change. The second pulse arrives after half period of oscillation at  $+3/2 \leftrightarrow -3/2$  transition. The condition  $B = B^*$  means that the transition  $+1/2 \leftrightarrow -1/2$  experienced odd number of half oscillations. Thus both coherent superpositions that were bright for the first pulse, become dark for the second one and vice versa. Consequently, the second pulse “sees” the medium in which there are two ground states having populations of 1/4 (former dark states), two excited states  $\pm\bar{E}$  having populations  $1/4(2+x)$ , and two  $\pm 2\bar{A}$  states coupled to the  $\pm\bar{E}$  ones by phonon relaxation. Thus the second pulse redistributes the populations in the following way:

$$\rho_{\bar{E}\bar{E}} = \frac{3+2x}{4(2+x)^2} = \rho_{B'_{1,2} B'_{1,2}},$$

$$\rho_{2\bar{A}2\bar{A}} = x\rho_{\bar{E}\bar{E}}, \quad \rho_{D'_{1,2} D'_{1,2}} = \frac{1}{4(2+x)}. \quad (20)$$

Here  $B'_{1,2}$  and  $D'_{1,2}$  denote the two bright and two dark states for the second pulse, respectively. The populations of the for ground-state sublevels are given by the following expression:

$$\rho_{\pm 1/2 \pm 1/2, \pm 3/2 \pm 3/2} = (\rho_{B'_{1,2} B'_{1,2}} + \rho_{D'_{1,2} D'_{1,2}})/2 = \frac{5+3x}{8(2+x)^2}. \quad (21)$$

Thus it is possible to get population inversion at the  $R_2$  transition if the following condition is satisfied:

$$\rho_{2\bar{A}2\bar{A}} = \frac{x(3+2x)}{4(2+x)^2} > \rho_{\pm 1/2 \pm 1/2, \pm 3/2 \pm 3/2}$$

$$= \frac{5+3x}{8(2+x)^2}, \quad x > x_{crit} = \frac{\sqrt{89}-3}{8} \approx 0.804. \quad (22)$$

For room-temperature ruby,  $x = 0.87 > x_{crit}$ , thus population inversion can be achieved. Under the optimal conditions, the population of  $\pm 2\bar{A}$  states can be made  $\approx 0.125$  while the population of each of the four ground-state Zeeman sublevels is  $\approx 0.115$ . This result is obtained under the condition of correlated action of the coherences at two independent spin transitions. Of course, it is required that the time interval

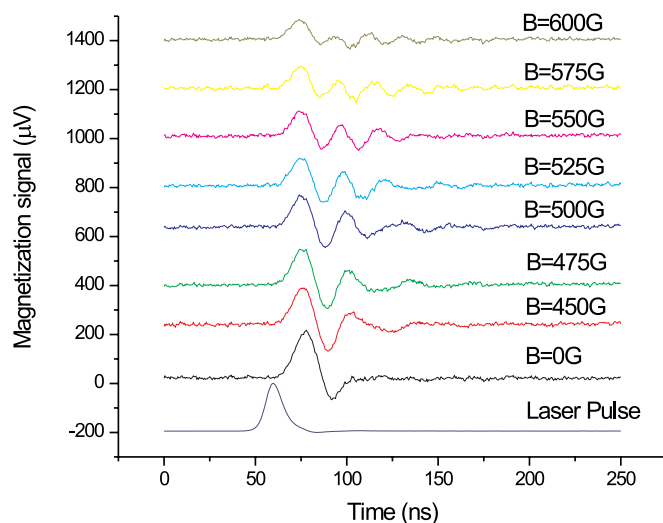


FIG. 4. (Color online) Laser-induced emf in room-temperature ruby crystal. The frequency of magnetization oscillations alters as the external magnetic field changes.

between the two pulses is shorter than the shortest decay time of those two coherences.

#### IV. EXPERIMENTAL OBSERVATION OF RAMSEY FRINGES IN RUBY

In this section, experimental results on observation of Ramsey fringes in CPT spectrum of a room-temperature ruby crystal are presented. Spin coherence was excited at Zeeman transition  $+3/2 \leftrightarrow -3/2$  by means of a circularly polarized pulsed Ti:sapphire laser tuned in resonance with the ruby  $R_1$  line. The behavior of Zeeman coherence was tested in the preceding experiment, in which oscillations of laser-induced magnetization were observed. In that experiment, a ruby crystal was placed into an external magnetic field produced by an electromagnet whose direction was perpendicular to the crystal axis. Circularly polarized laser output (about 1 mJ per pulse, 84 Hz repetition rate) was loosely focused onto the ruby sample and propagated along the crystal axis. A single turn pickup coil, whose axis coincided with the  $c$  axis, was used to detect the magnetization. The emf signal was amplified by a 24-dB broadband amplifier (500 MHz bandwidth) and passed through a low-pass filter (3 dB at 55 MHz) in order to filter out high-frequency noise (mostly, FM radio stations operating at  $\approx 100$  MHz). The resulting signal was averaged several thousand times using a digital oscilloscope (Tektronix TDS684A). The results of these measurements are shown in Fig. 4. The laser-induced origin of these oscillations was confirmed by changing laser polarization from  $\sigma^+$  to  $\sigma^-$  and observation of the signal sign change. The frequency of magnetization oscillations depends on the external magnetic field in accordance with cubic dependence of the frequency splitting between  $\pm 3/2$  states. This measurement basically repeats the result obtained in [15] in a slightly more systematic manner.

The above auxiliary test clearly indicates the presence of oscillating ground-state coherence. After that, observation of

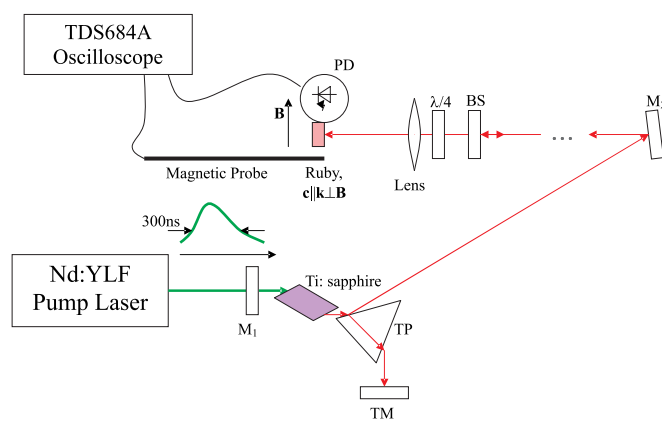


FIG. 5. (Color online) Experimental setup used in observation of Ramsey fringes in ruby. Ti:sapphire laser cavity is formed by mirror ( $M_1$ ), tuning prism (TP), and tuning mirror (TM). Output of the laser system for three distances between the primary oscillator and the beam splitter (BS) is shown in Fig. 6. Laser-induced fluorescence detected by a photodiode (PD) is studied as a function of the external magnetic field.

Ramsey fringes in the CPT spectrum of ruby was performed in the following manner (see Fig. 5). A short-cavity Ti:sapphire laser operating in the free-running mode was pumped with the second harmonic of a Nd:YLF laser (527 nm) having a rather long pulse ( $\sim 300$  ns). The Ti:sapphire laser emitted a short pulse ( $\approx 4.5$  ns at 694.3 nm) before the pump pulse ended. After traveling several meters, the beam from a Ti:sapphire laser was split on a 50%/50% beamsplitter. Half of the beam was sent back into the laser cavity while the other half was circularly polarized by  $\lambda/4$  waveplate and focused onto the ruby crystal placed inside an electromagnet. The first half of the beam (the one sent back into the laser) served as a seeding pulse for the laser. As a result, a train of several 4.5-ns laser pulses separated by a few tens of nanoseconds was generated. The typical shape of the train observed with a 1.5-GHz-bandwidth photodiode and 500-MHz-bandwidth oscilloscope is shown in Fig. 6. The time interval between the pulses in the train was controlled by the distance between the beamsplitter and the short laser cavity. It was chosen to be longer than the Zeeman decoherence time so that only two subsequent pulses contribute to the interference pattern. In other words, the medium does not “remember” the phase of Zeeman coherence created by the first pulse at the arrival of the third, fourth, and later pulses. The beam size at the location of the ruby crystal was 50–100  $\mu\text{m}$  and the total energy in the train was 0.5–1 mJ. The repetition rate of the pump laser was 84 Hz, so that the time interval between the subsequent trains ( $\sim 12$  ms) was much longer than the population decay time of the excited optical state. This was done in order to make sure that before each pulse train chromium ions inside ruby crystals are in the same initial state (ground state). Laser-induced ruby fluorescence (i.e., population of the excited optical states) was detected by a photodiode 1 ms after the laser pulse during 100  $\mu\text{s}$ . The photodiode signal was stored in a sample-and-hold system and plotted as a function of the sweeping external magnetic field applied to the crystal. The sweep rate was

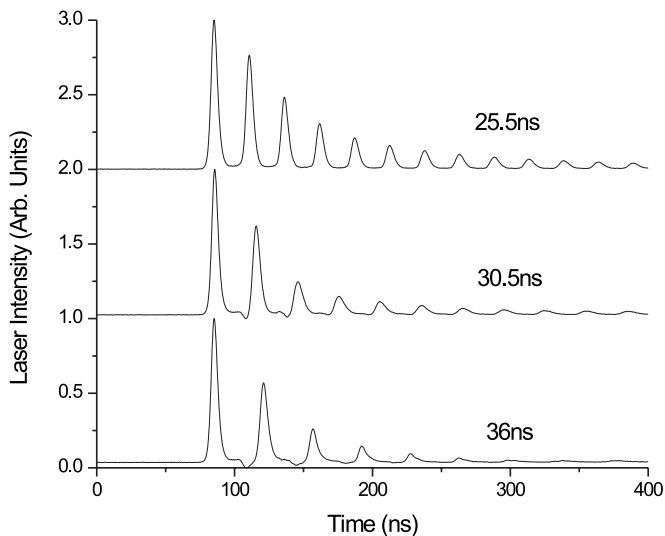


FIG. 6. Shapes of the three pulse trains for three different distances between the beamsplitter and the short laser cavity. See text for details.

chosen to be 0.16 Hz, so that it was much slower than the laser repetition rate. The signal was averaged over several hundred sweeps of the magnetic field.

The results of three measurements for three distances between the beamsplitter and the short laser cavity (i.e., for three repetition rate of pulses in the train) are shown in Fig. 7. The upper graph shows bare spectra, i.e., the fluorescence intensity as a function of the magnetic field. The lower traces show the same spectra recalculated into frequency domain. In the latter re-scaling procedure, it was assumed that the external magnetic field was exactly perpendicular to the crystal axis. Under this condition, the frequency splitting between levels  $\pm 3/2$  in the vicinity of zero field is given by the following formula:

$$\nu_{3/2 \leftrightarrow -3/2} = \frac{3}{8} \left( \frac{g_{\perp} \mu_B B}{\hbar D} \right)^3 D. \quad (23)$$

Periodic modulation of a single pulse CPT spectrum due to the action of the second pulse is clearly seen in Fig. 7. Even though it was not possible to determine the positions of fringes exactly because of rather poor signal-to-noise ratio, one sees that these positions roughly correspond to the repetition rates of pulses in the trains (28, 33, and 39 MHz, respectively).

The quality of the CPT spectrum and its modulation could be significantly improved if the laser emitting a single pulse of 100-ps–1-ns duration was available. Exploiting such a laser would allow us to use shorter pulse delays  $T \sim 3\text{--}5 \text{ ns} \ll \gamma^{-1}$  so that the interference pattern is more pronounced.

## V. CONCLUSION

The following is the summary of the results obtained in the paper. Coherent population trapping (CPT) in a three-

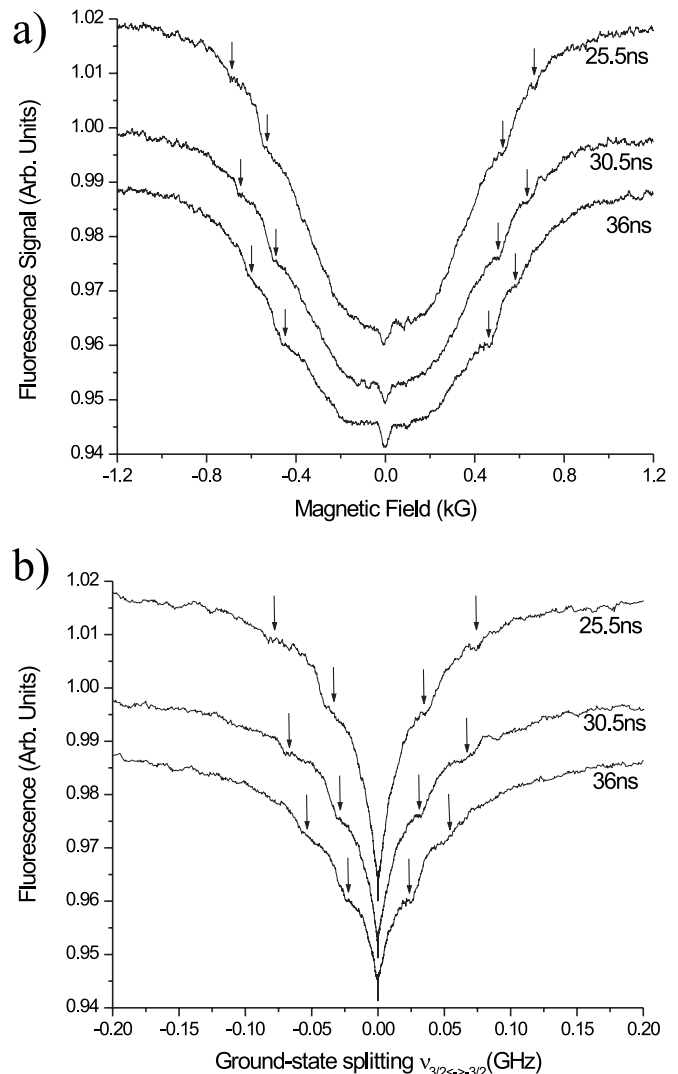


FIG. 7. (a) CPT spectra of ruby under excitation by a train of pulses. Fluorescence is plotted as a function of the magnetic field. The three spectra correspond to the pulse trains shown in Fig. 6. The sharp CPT resonance at zero magnetic field corresponds to the  $\Lambda$ -system coupling  $\pm 1/2$  states and should be disregarded. (b) Same spectra recalculated into frequency domain. Crystal axis is assumed to be exactly perpendicular to the magnetic field, so that the splitting between levels  $\pm 3/2$  is equal to  $3g_{\perp}^3 \mu_B^3 B^3 / 8\hbar^3 D^2$ . For both (a) and (b) arrows indicate the positions of resonances of reduced fluorescence excitation.

level medium under the action of two optical pulses is considered under the condition of no population return from the excited optical state to the ground-state sublevels. The situation is typical for optical crystals doped with rare-earth and transition-metal ions at room temperature. Periodic modulation of optical excitation as a function of either pulse delay or ground-state splitting due to Ramsey interference is predicted. The period of modulation in the frequency domain is inversely proportional to the time interval between the pulses. An interesting possibility of creating population inversion in such a system is revealed for the two pulses saturating the optical transition and delayed by half period of

ground-state splitting. Such population inversion does not require the use of optical pulses of certain area ( $\pi$  pulses). If applied to ruby at room temperature, such a method would allow one to create population inversion at the  $R_2$  transition (692.9 nm) under optical excitation at the  $R_1$  transition of lower frequency (694.3 nm); experimental observation of Ramsey fringes in the CPT spectrum of room-temperature ruby is reported. Laser-induced fluorescence oscillates as a

function of the ground-state splitting and the oscillation period corresponds to the time interval between the pulses.

#### ACKNOWLEDGMENTS

The authors gratefully acknowledge P. Hemmer, Y. Rostovtsev, E. Kuznetsova, F. Vagizov, K. Hakuta, and V. Sautenkov for useful discussions. This work was supported by NSF and AFOSR.

- 
- [1] N. F. Ramsey, *Rev. Mod. Phys.* **62**, 541 (1990).
  - [2] E. Arimondo, in *Progress in Optics*, edited by E. Wolf (Elsevier Science, Amsterdam, 1996), Vol. 35, p. 257.
  - [3] J. E. Thomas, P. R. Hemmer, S. Ezekiel, C. C. Leiby, Jr., R. H. Picard, and C. R. Willis, *Phys. Rev. Lett.* **48**, 867 (1982); P. R. Hemmer, M. S. Shahriar, H. Lamela-Rivera, S. P. Smith, B. E. Bernacki, and S. Ezekiel, *J. Opt. Soc. Am. B* **10**, 1326 (1993).
  - [4] T. Zanon, S. Guerandel, E. de Clercq, D. Holleville, N. Dimarcq, and A. Clairon, *Phys. Rev. Lett.* **94**, 193002 (2005); A. S. Zibrov and A. B. Matsko, *Phys. Rev. A* **65**, 013814 (2001).
  - [5] Y. Xiao, I. Novikova, D. F. Phillips, and R. L. Walsworth, *Phys. Rev. Lett.* **96**, 043601 (2006).
  - [6] D. Budker, W. Gawlik, D. F. Kimball, S. M. Rochester, V. V. Yashchuk, and A. Weis, *Rev. Mod. Phys.* **74**, 1153 (2002).
  - [7] S. Stuffer, P. Ester, A. Zrenner, and M. Bichler, *Phys. Rev. Lett.* **96**, 037402 (2006).
  - [8] D. Vion, A. Aassime, A. Cottet, P. Joyez, H. Pothier, C. Urbina, D. Esteve, and M. H. Devoret, *Fortschr. Phys.* **51**, 462 (2003).
  - [9] R. Kolesov, *Phys. Rev. A* **72**, 051801(R) (2005).
  - [10] O. A. Kocharovskaya and Ya. I. Khanin, *Zh. Eksp. Teor. Fiz.* **90**, 1610 (1986) [*Sov. Phys. JETP* **63**, 945 (1986)]; V. A. Sautenkov *et al.*, *Phys. Rev. A* **71**, 063804 (2005).
  - [11] R. Orbach, *Proc. R. Soc. London, Ser. A* **264**, 458 (1961).
  - [12] T. H. Maiman, R. H. Hoskins, I. J. D'Haenens, C. K. Asawa, and V. Evtuhov, *Phys. Rev.* **123**, 1151 (1961).
  - [13] S. Sugano and Y. Tanabe, *J. Phys. Soc. Jpn.* **13**, 880 (1958); M. O. Schweika-Kresimon, J. Gutschank, and D. Suter, *Phys. Rev. A* **66**, 043816 (2002).
  - [14] Y. Fukuda, Y. Takagi, and T. Hashi, *Phys. Lett.* **48A**, 183 (1974); Y. Takagi, Y. Fukuda, and T. Hashi, *Opt. Commun.* **55**, 115 (1985).
  - [15] Y. Takagi, Y. Fukuda, K. Yamada, and T. Hashi, *J. Phys. Soc. Jpn.* **50**, 2672 (1981).
  - [16] J. C. Walling, H. P. Jenssen, R. C. Morris, E. W. O'Dell, and O. G. Peterson, *Opt. Lett.* **4**, 182 (1979).